SUPPLEMENTARY MATERIAL
Air sheet contraction

Zhen Jian[1]†, Peng Deng[1]† and Marie-Jean Thoraval[1]‡

[1]State Key Laboratory for Strength and Vibration of Mechanical Structures, International Center for Applied Mechanics, School of Aerospace, Xi'an Jiaotong University, Xi'an 710049, P. R. China

CONTENTS

† These authors contributed equally to this work.
‡ Email address for correspondence: mjthoraval@xjtu.edu.cn

S1. Complete range of Ohnesorge numbers

Figures including the full range of *Oh* are added here for reference, in Fig. S1 for Fig. 2, Fig. S2 for Fig. 8(d), Fig. S3 for Fig. 10 and Fig. S4 for Fig. 14.

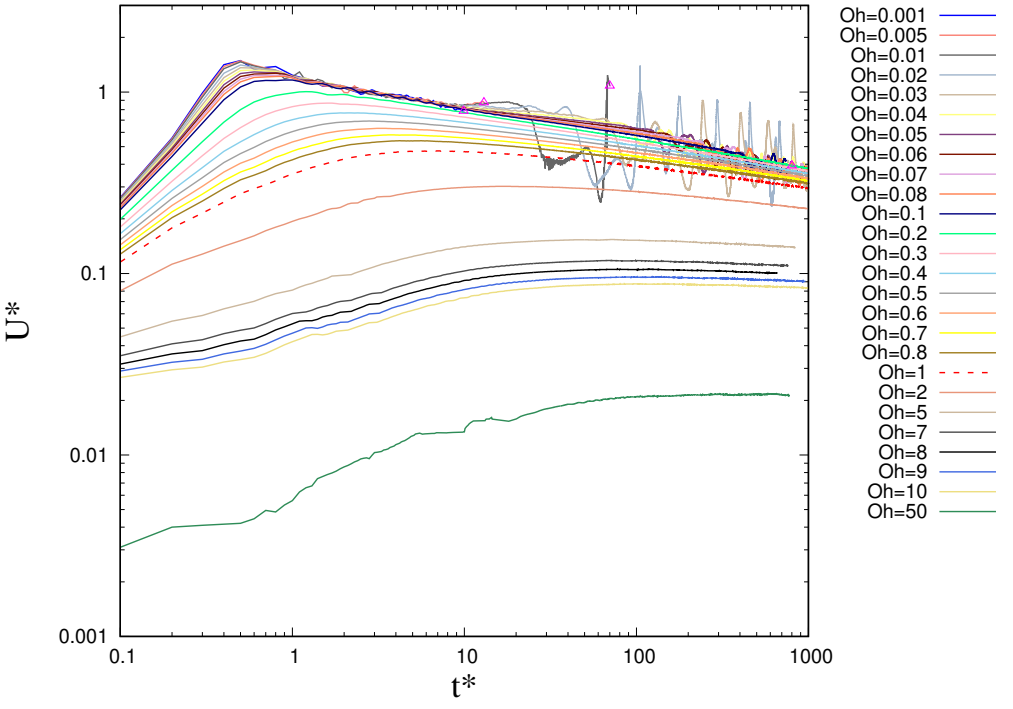

FIGURE S1. [Extended Fig. 2 from the manuscript.] Contraction velocity of the rim U^* versus time t^* in log-log scale for the full range of Ohnesorge number. The data after pinch-off are not plotted, and the pinch-off time is indicated by empty triangle. Dashed line is used for $Oh = 1$ for clear view and $U^* = U/U_\rho$, $t^* = t/\tau_\rho$.

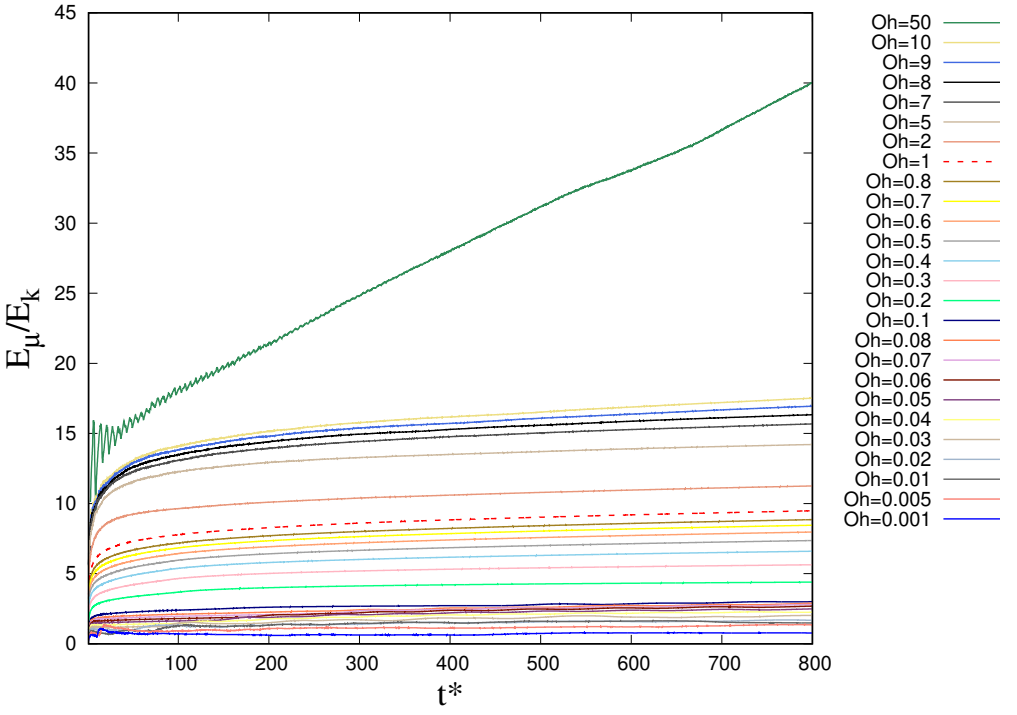

FIGURE S2. [Extended Fig. 8(d) from the manuscript.] Ratio between viscous dissipation (E_μ) and kinetic energy (E_k) versus time t^* for the full range of Ohnesorge number. Dashed line is used for $Oh = 1$ for clear view and $t^* = t/\tau_\rho$.

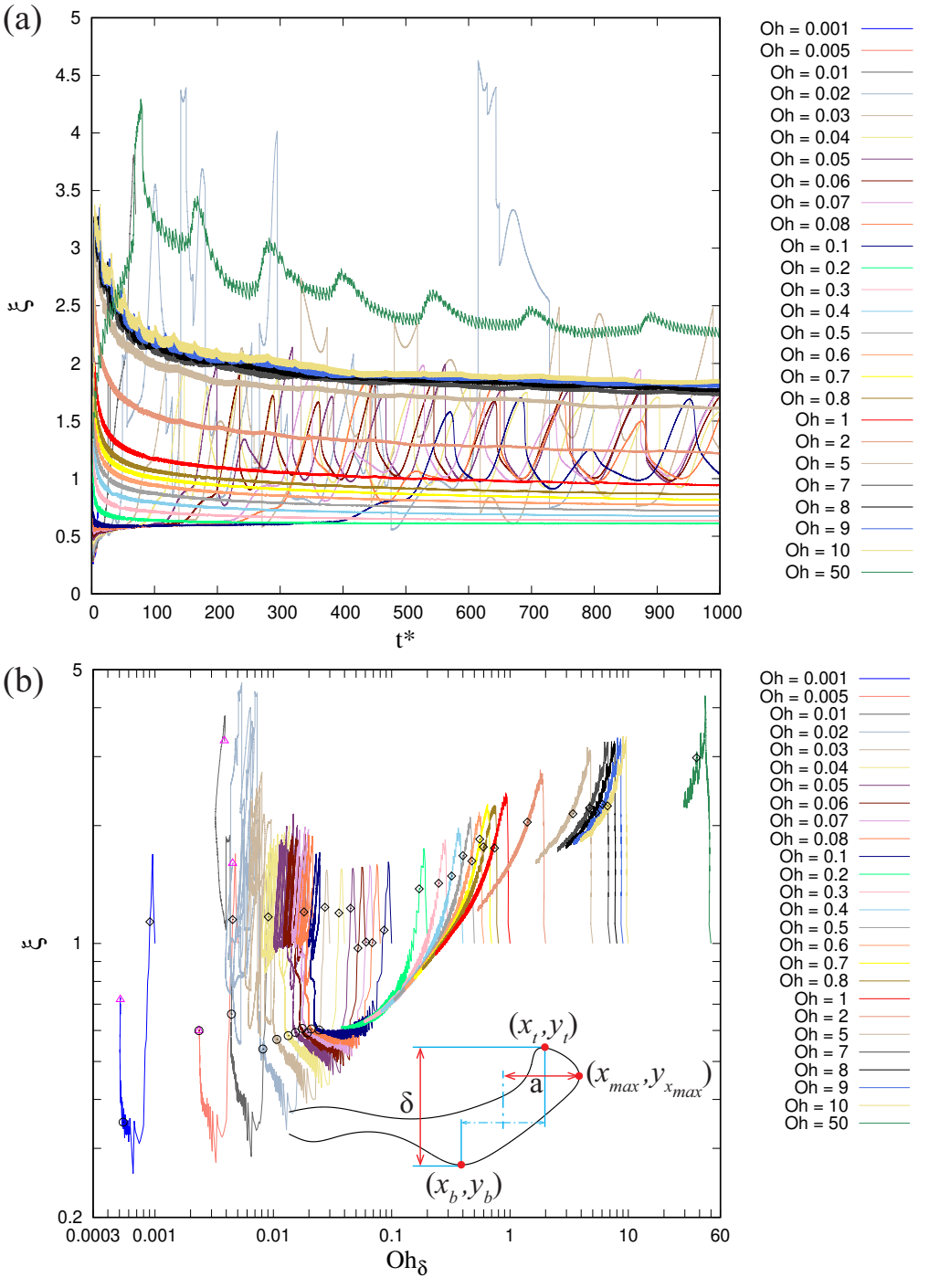

FIGURE S3. [Extended Fig. 10 from the manuscript.] (a) Aspect ratio of the rim ξ versus time in normal scale and (b) Aspect ratio of the rim ξ versus local Ohnesorge number Oh_δ in log-log scale for the full range of Ohnesorge number. The aspect ratio ξ corresponding to the maximum contraction velocity is indicated by an empty diamond, the aspect ratio ξ corresponding to the starting time of the oscillations is indicated by an empty circle, the aspect ratio ξ corresponding to the time of pinch-off is indicated by an empty triangle and the data after pinch-off are not plotted for $Oh \leqslant 0.02$ in (b). Inset shows the definition of the aspect ratio $\xi = 2a/\delta$ and the rim profile is taken from $Oh = 0.05$ at $t^* = 175$. $t^* = t/\tau_\rho$.

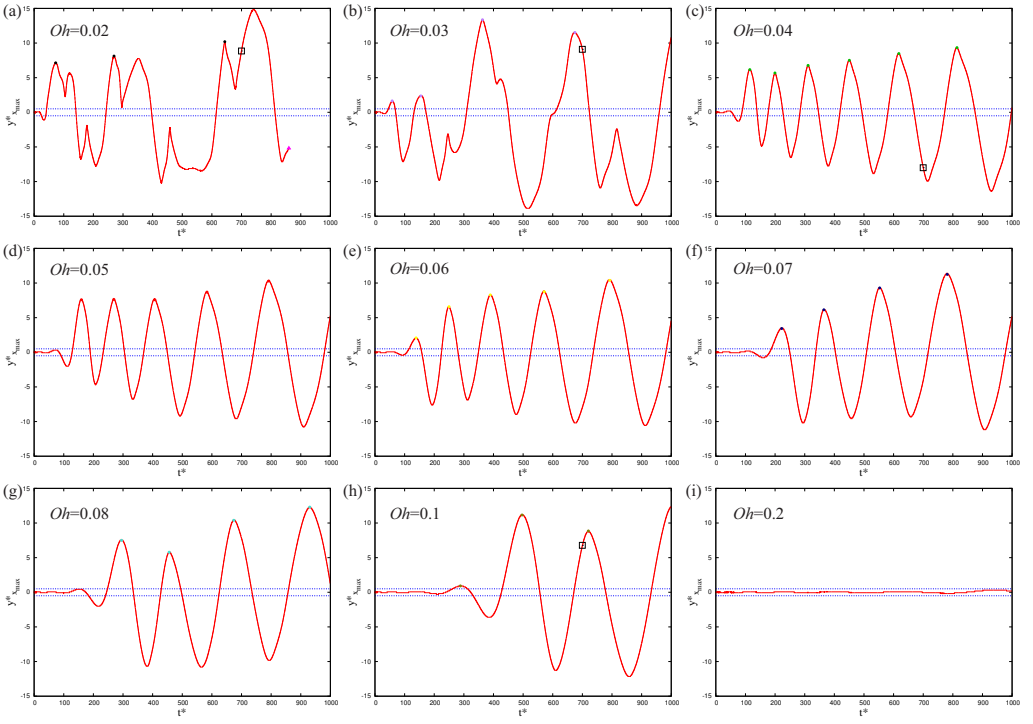

FIGURE S4. [Extended Fig. 14 from the manuscript.] Y-coordinate of the x-maximum point of the rim $y^*_{x_{max}}$ versus time t^* at (a) $Oh = 0.02$, (b) $Oh = 0.03$, (c) $Oh = 0.04$, (d) $Oh = 0.05$, (e) $Oh = 0.06$, (f) $Oh = 0.07$, (g) $Oh = 0.08$, (h) $Oh = 0.1$ and (i) $Oh = 0.2$. Horizontal dashed lines indicate the threshold of oscillation $y^* = 0.5$ and $y^* = -0.5$. Filled circles indicate the boundaries of a period used to calculate the average Strouhal number $\overline{St}$ and different colour is used for different Ohnesorge number as in Fig. 15. The data after pinch-off are not plotted for $Oh = 0.02$ (Pinch-off time is indicated by empty triangle at $t^* = 862.5$). $Oh = 0.2$ is plotted for comparison and it is no-oscillating according to the definition $|y^*_{x_{max}}| < 0.5$. $y^* = y/e$ and $t^* = t/\tau_\rho$.

S2. Influence of simulations parameters

S2.1. *Domain size*

We test a double-sized domain (Fig. S5b) to compare it with the domain used in the paper (Fig. S5a), keeping the same initial dimension of the air sheet. The refinement level for the double-sized domain is set to one level higher (smallest cells twice smaller) to maintain the same refinement of the air sheet.

As shown in Fig. S6, the velocity curves agree well and the scaling law of the contraction velocity is valid for the two domain sizes. The relative error of the maximum contraction velocity

$$\varepsilon_{domain} = \frac{U_{max-double-size} - U_{max-paper}}{U_{max-double-size}}$$

is $\varepsilon_{domain} = 0.016\%, 0.23\%, 0\%$ at $Oh = 0.05, 0.1, 0.2$ respectively, which can be neglected.

A time shift is observed on the velocity oscillation, but the period of the oscillation (or the frequency) and the profile of the oscillation are similar (Fig. S6(a,b)). Therefore, the domain size used in the paper (Fig. S5a) is large enough to avoid boundary effects and is also small enough to save computing time.

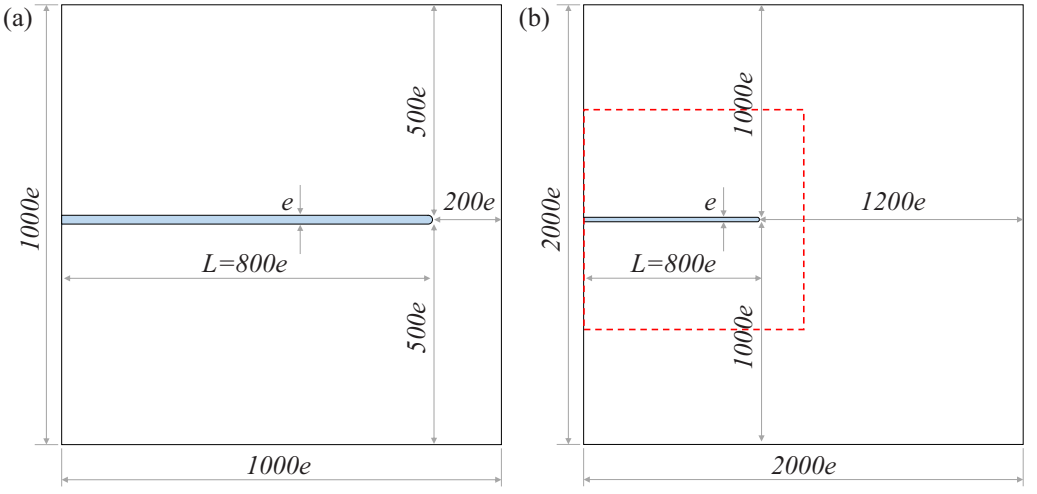

FIGURE S5. Sketch of (a) domain used in the paper and (b) double-sized domain. The red dashed line represents the domain used in the paper as in (a). The sketch is not on scale.

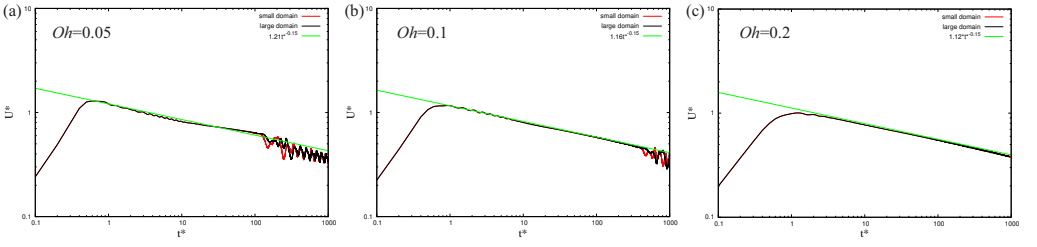

FIGURE S6. Contraction velocity of the rim U^* versus time t^* for the two domain sizes defined in Fig. S5 in log-log scale at (a) $Oh = 0.05$, (b) $Oh = 0.1$ and (c) $Oh = 0.2$. The scaling law of the contraction velocity is (a) $U^* = 1.21t^{*-0.15}$, (b) $U^* = 1.16t^{*-0.15}$ and (c) $U^* = 1.12t^{*-0.15}$. Red corresponds to small domain as Fig. S5(a) and black corresponds to large domain as Fig. S5(b). $U^* = U/U_\rho$ and $t^* = t/\tau_\rho$.

S2.2. *Initial profile*

In our simulations, the end of the air sheet is initially connected to a half-circle. The parallel lines of the sheet are tangent to the half-circle at the connection point. They are mathematically continuous and first order derivable at the connection point. A similar configuration was also used in previous studies such as Fig. 1 in Song & Tryggvason (1999), Fig. 1 in Sünderhauf *et al.* (2002) and Fig. 2 in Gordillo *et al.* (2011).

The finite jump of curvature at the connection point does not affect the simulations, as it is immediately smoothed by the curvature calculations of the VOF interface reconstruction. To check the effect of the curvature jump, we tested a new initial profile $|x|^{2.01}+|y|^{2.01}=0.5^{2.01}$ for the tip of the sheet, with continuous curvature at the connection point with parallel lines. The difference of profile between a circle $x^2+y^2=0.5^2$ and $|x|^{2.01}+|y|^{2.01}=0.5^{2.01}$ is negligible (Fig. S7a). The relative error of the maximum contraction velocity

$$\varepsilon_{ip}=\frac{U_{max-2.01}-U_{max-circle}}{U_{max-2.01}}$$

is $\varepsilon_{ip}=0.33\%$ at $Oh=0.1$.

The velocity curve agrees well even in the oscillation part and the scaling law of the contraction velocity $U^*=1.16t^{*-0.15}$ is valid for both initial profiles (Fig. S7b). Therefore, the effect of curvature jump at the connection between the sheet and its half-circle end can be neglected.

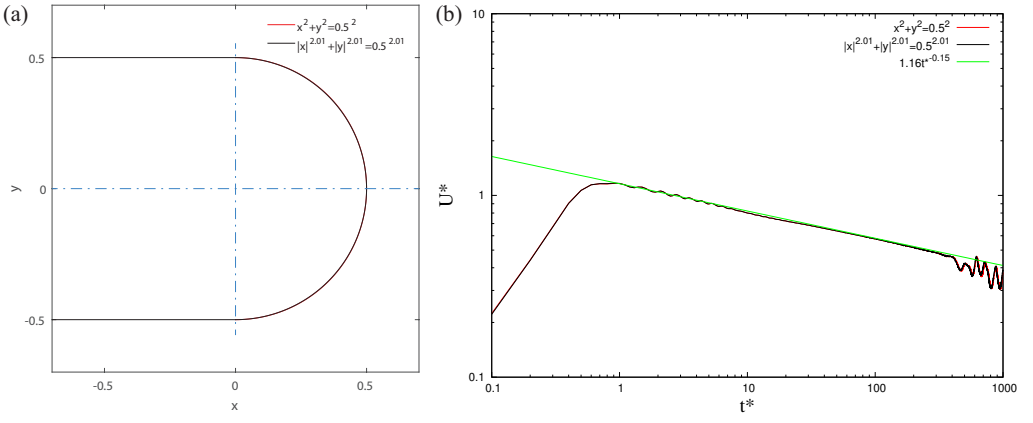

FIGURE S7. (a) Comparison of the profile between a circle $x^2+y^2=0.5^2$ and $|x|^{2.01}+|y|^{2.01}=0.5^{2.01}$. (b) Contraction velocity of the rim U^* versus time t^* for the initial profile with a half-circle and with the curve $|x|^{2.01}+|y|^{2.01}=0.5^{2.01}$ at $Oh=0.1$. The scaling law of the contraction velocity is $U^*=1.16t^{*-0.15}$. Red corresponds to circle and black corresponds to $|x|^{2.01}+|y|^{2.01}=0.5^{2.01}$. $U^*=U/U_\rho$ and $t^*=t/\tau_\rho$.

S2.3. *Refinement level*

We test a higher refinement level 14 compared to the level 13 used in the paper. As shown in Fig. S8, the relative error of the maximum contraction velocity

$$\varepsilon_{rl} = \frac{U_{max-l14} - U_{max-l13}}{U_{max-l14}}$$

is $\varepsilon_{rl} = 3.9\%, 6.1\%, 6.6\%$ at $Oh = 0.05, 0.1, 0.2$ respectively. The scaling law of the contraction velocity is valid for the two levels.

Some deviations are observed on the velocity oscillations (Fig. S8a,b), suggesting that the oscillations could appear earlier with more refined simulations. Indeed, the oscillations are connected to the vorticity production at the interface, over a thin boundary layer that is challenging to capture accurately. However, the main features studied in the paper are still valid. It takes about 7 days on 28 processors for the simulation of $Oh = 0.05$ at level 14 and the computing time increases dramatically when the Ohnesorge number increases. Therefore, the level 13 used in the paper is a good compromise for this systematic study on the air film contraction.

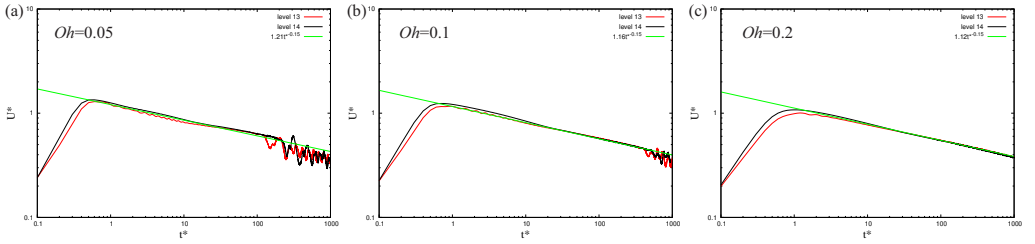

FIGURE S8. Contraction velocity of the rim U^* versus time t^* for different refinement levels 13 and 14 in log-log scale at (a) $Oh = 0.05$, (b) $Oh = 0.1$ and (c) $Oh = 0.2$. The scaling law of the contraction velocity is (a) $U^* = 1.21t^{*-0.15}$, (b) $U^* = 1.16t^{*-0.15}$ and (c) $U^* = 1.12t^{*-0.15}$. Red corresponds to level 13 and black corresponds to level 14. $U^* = U/U_\rho$ and $t^* = t/\tau_\rho$.

S3. Rim geometry (see Sec. 4.1. Rim geometry in the paper)

Fig. S9 shows the comparison of the rim profiles rescaled by $t^{*0.425}$, obtained from the scaling $U^* \sim t^{*-0.15}$ as presented in Fig. 9(b,d,f), and the profiles rescaled by $t^{*0.4}$, that would be predicted by a constant drag coefficient theory with $U^* \sim t^{*-0.2}$ as previously observed by Mirjalili *et al.* (2018). A slightly better collapse is observed with the scaling by $t^{*0.425}$, which is consistent with the $U^* \sim t^{*-0.15}$ observed on the contraction velocity.

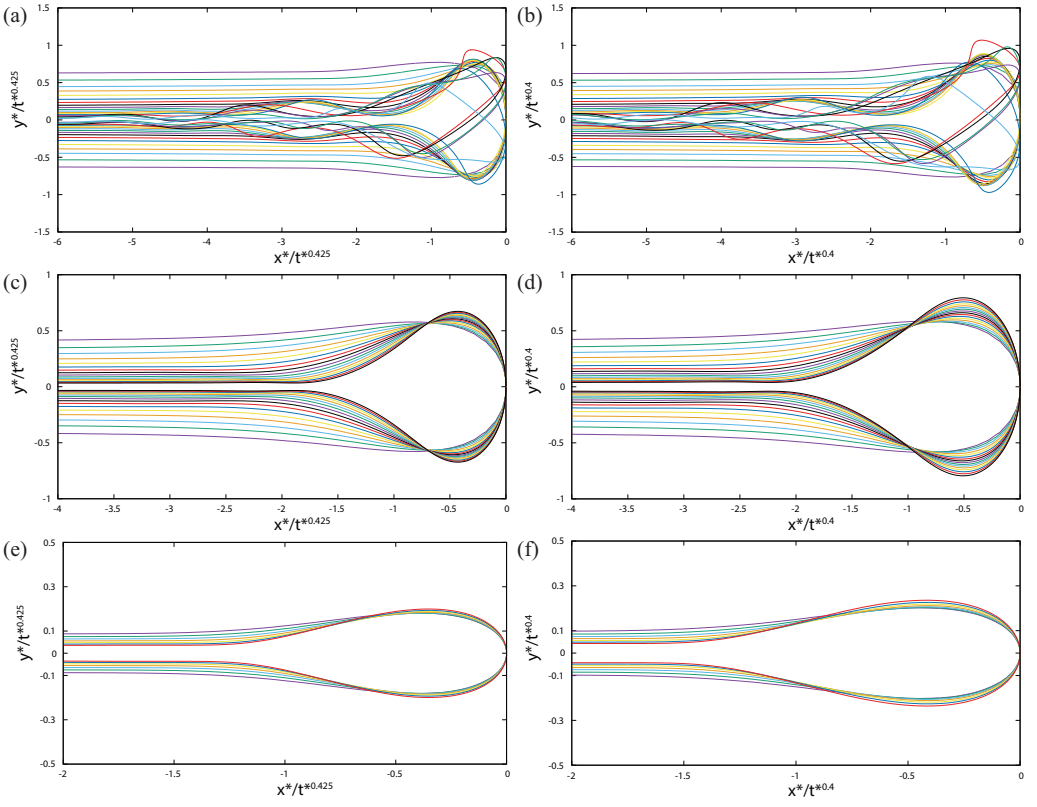

FIGURE S9. (a,c,e) Translated rim profiles rescaled by $t^{*0.425}$ as in Fig. 9(b,d,f), and (b,d,f) translated rim profiles rescaled by $t^{*0.4}$ in the decreasing phase of the contraction velocity for three regimes: vortex-shedding regime (a,b, $Oh = 0.05$), smooth-contraction regime (c,d, $Oh = 0.3$) and viscous regime (e,f, $Oh = 7$). A logarithmic progression of time is used to choose the profiles, where $t^*_{n+1} = 1.5t^*_n$. The first profile is plotted at the time of maximum contraction velocity $t^*_1 = t^*_{U^*_{max}}$. The time of the first and last profiles is: $t^*_1 = 0.6$, $t^*_{19} = 886.7$, at $Oh = 0.05$; $t^*_1 = 1.7$, $t^*_{16} = 744.4$, at $Oh = 0.3$ and $t^*_1 = 71.4$, $t^*_7 = 813.3$, at $Oh = 7$. $x^* = x/e$, $y^* = y/e$ and $t^* = t/\tau_\rho$.

REFERENCES

GORDILLO, L., AGBAGLAH, G., DUCHEMIN, L. & JOSSERAND, C. 2011 Asymptotic behavior of a retracting two-dimensional fluid sheet. *Phys. Fluids* **23** (12), 122101.

MIRJALILI, S., CHAN, W. H. R. & MANI, A. 2018 High Fidelity Simulations of Micro-Bubble Shedding from Retracting Thin Gas Films in the Context of Liquid-Liquid Impact. In *32nd Symposium on Naval Hydrodynamics*.

SONG, M. & TRYGGVASON, G. 1999 The formation of thick borders on an initially stationary fluid sheet. *Phys. Fluids* **11** (9), 2487–2493.

SÜNDERHAUF, G., RASZILLIER, H. & DURST, F. 2002 The retraction of the edge of a planar liquid sheet. *Phys. Fluids* **14** (1), 198–208.